Autonomous Automobile Trajectory Tracking for Off-Road Driving: Controller Design, Experimental Validation and Racing[†]

Gabriel M. Hoffmann, Claire J. Tomlin
Department of Aeronautics and Astronautics
Stanford University
Stanford, CA 94305, USA
{gabeh,tomlin}@stanford.edu

Michael Montemerlo, Sebastian Thrun
Computer Science Department
Stanford University
Stanford, CA 94305, USA
{mmde,thrun}@stanford.edu

***Abstract*— This paper presents a nonlinear control law for an automobile to autonomously track a trajectory, provided in real-time, on rapidly varying, off-road terrain. Existing methods can suffer from a lack of global stability, a lack of tracking accuracy, or a dependence on smooth road surfaces, any one of which could lead to the loss of the vehicle in autonomous off-road driving. This work treats automobile trajectory tracking in a new manner, by considering the orientation of the front wheels – not the vehicle's body – with respect to the desired trajectory, enabling collocated control of the system. A steering control law is designed using the kinematic equations of motion, for which global asymptotic stability is proven. This control law is then augmented to handle the dynamics of pneumatic tires and of the servo-actuated steering wheel. To control vehicle speed, the brake and throttle are actuated by a switching proportional integral (PI) controller. The complete control system consumes a negligible fraction of a computer's resources. It was implemented on a Volkswagen Touareg, "Stanley", the Stanford Racing Team's entry in the DARPA Grand Challenge 2005, a 132 mi autonomous off-road race. Experimental results from Stanley demonstrate the ability of the controller to track trajectories between obstacles, over steep and wavy terrain, through deep mud puddles, and along cliff edges, with a typical root mean square (RMS) crosstrack error of under 0.1 m. In the DARPA National Qualification Event 2005, Stanley was the only vehicle out of 40 competitors to not hit an obstacle or miss a gate, and in the DARPA Grand Challenge 2005 Stanley had the fastest course completion time.**

I. Introduction

Autonomous automobile technology is a rapidly developing field, with interest in both academia and industry. A historical emphasis in driving control system design has considered motion on paved, uniform surfaces, yielding many high performance systems. There has been increasing interest in making vehicles also capable of autonomous off-road driving. Driving on such terrain poses additional challenges. The control system must be able to handle rough and curvy roads, and quickly varying terrain types, such as gravel, loose sand, and mud puddles – while stably tracking trajectories between closely spaced hazards. The vehicle must be able to recover from large disturbances, without intervention.

This paper addresses these challenges by presenting a nonlinear control law for an automobile to autonomously track a trajectory, provided in real-time, on rapidly varying, off-road terrain. Automobile trajectory tracking is treated in a new way, by considering the orientation of the front wheels – not the vehicle's body – with respect to the desired trajectory, enabling collocated control of the system. A control law is designed using the kinematic equations of motion, for which global asymptotic stability is proven. It is then augmented to handle the dynamics of pneumatic tires and of the servo-actuated steering wheel. To control vehicle speed, the brake and throttle are actuated by a switching proportional integral (PI) controller. The controller consumes a negligible fraction of a computer's resources. It was implemented on an autonomous Volkswagen Touareg, "Stanley", the Stanford Racing Team's entry in the DARPA Grand Challenge 2005, a 132 mile off-road race without a human in the vehicle. Using this controller, Stanley had the fastest completion time in the race, averaging 19.1 mph. Results from hundreds of miles of testing demonstrate the ability of the controller to track trajectories between obstacles, over steep and wavy terrain, through deep mud puddles, and along cliff edges, with a typical root mean square (RMS) crosstrack error of under 0.1 m. The top speed tested on Stanley was 42 mph on a dirt road, an upperbound of speed needed to race. Stanley's successor for the DARPA Urban Challenge, a Passat named "Junior", used the controller to drive 71 mph at Moffett Field.

Fig. 1. Stanley, the Stanford Racing Team's entry in the DARPA Grand Challenge 2005, under autonomous control, with no human in the vehicle.

For on-road automobile driving, many researchers have used the bicycle model with linearized states to design trajectory tracking controllers with consideration for the pneumatic tires[1]. For instance, in [2], the GMC Jimmy was controlled with a PID controller, with the linearized system

[†] The Stanford Racing Team was supported by Primary Supporters: Volkswagen of America's Electronics Research Lab, Mohr Davidow Ventures, Android, and Red Bull. The SRT also received support from Intel Research, Honeywell, Tyzx, Inc., and Coverity, Inc. Generous financial contributions were made by David Cheriton, the Johnson Family, and Vint Cerf.

dynamics proven robustly stable. In experiments, it exhibited tight tracking up to 25 mph. In the California PATH project, a linear controller was used, and demonstrated tracking up to 78 mph[3]. Demonstrations were given of driving 7.6 mi autonomously on the highway, reaching 60 mph, using magnetic markers for tracking. The lateral control law used a lookahead distance for the error metric[4]. A motivation for using lookahead distance is given in [5]. Lookahead distance was also used in [6], with potential fields, to provide driver assistance steering. Without driver intervention, this steering assistance controller has more error on curves than previous systems, but bounds on this error are proven[5]. It was tested at up to 50 mph. Although these on-road control laws have achieved excellent accuracy, they are not designed for an off-road environment. The vehicle must be able to recover from large disturbances that would violate assumptions used for linearization based methods.

There have been a number of recent off-road driving projects. The NIST HMMWV has driven off-road at speeds up to 22 mph, using clothoid trajectories to parameterize a predictive controller[7]. It tracks the resulting trajectories in open loop[8]. The system was demonstrated in a rolling grassy field with trees. Tracking error increased with speed, so required clearance distance from obstacles also increased with speed. Another popular technique for off-road driving has been controllers that "chase" a goal point using a PID controller to point the front wheels toward a point ahead on the trajectory. Without heuristic functions, this controller is unstable at even moderate speeds, as discussed in [8]. It can clip corners, and have poor disturbance rejection. This technique has been successfully applied, including aboard many vehicles at the DARPA Grand Challenge 2005. These controllers have demonstrated poor performance in tight curves, and unpredictable crosstrack error, as exemplified by the results of the DARPA National Qualification Event 2005.

This paper proceeds by first presenting the two vehicle models used for controller design, kinematic and dynamic. Next, the trajectory tracking control laws are derived. Global asymptotic stability is proven for the kinematic control law. Finally, the results of months of field testing are given, with experimental data from hundreds miles of off-road driving.

II. Vehicle Models

This section describes two schemes used to model vehicle motion. The first is the kinematic model, which assumes the vehicle has negligible inertia. This permits design of a controller which is globally stable under that assumption. This assumption is effective for low speed driving[9]. The second is the dynamic model, which includes inertial effects: tire slip and steering servo actuation. This more complicated, but more accurate, scheme permits simulation for tuning and augmenting the controller to handle realistic dynamics.

A. Kinematic Model

The kinematic motion of an automobile, with speed $v(t)$, can be described with the crosstrack error, $e(t)$, of the guiding wheels, and the angle of those wheels with respect to the nearest segment of trajectory to be tracked, $(\psi(t)-\delta(t))$, as in Figure 2. Here, $\psi(t)$ is the yaw angle (heading) of the vehicle with respect to the closest trajectory segment, and $\delta(t)$ is the angle of the front wheels with respect to the vehicle. This reference frame allows the actuator to act directly on the error metric, yielding collocated sensing and control. For forward driving, the guiding wheels are the front wheels, and the derivative of the crosstrack error is

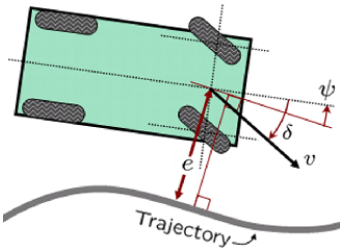

Fig. 2. Kinematic model of an automobile.

$$\dot{e}(t) = v(t)\sin(\psi(t)-\delta(t)) \tag{1}$$

where the steering is mechanically limited to $|\delta(t)| < \delta_{max}$. The derivative of the yaw angle, the yaw rate, is

$$\dot{\psi}(t) = r(t) = -\frac{v(t)\sin(\delta(t))}{a+b} \tag{2}$$

where a and b are the distance from the center of gravity (CG) to the front and rear wheels, respectively.

Note that for reverse driving, the rear wheels can be treated as the guiding wheels, yielding a useful parameterization that will be discussed in Section III-A.

B. Dynamic Model

To model the nonlinear dynamic motion of the vehicle, the effects of tire slip and of the steering servo motor are considered. The relevant states of the vehicle are depicted in Figure 3. The front and rear tire sets are modeled to each provide a force, $F_{yf}(t)$ and $F_{yr}(t)$, perpendicular to the rolling direction of the tire, and proportional to the angle, $\alpha(t)$, between the its local velocity vector and its forward direction. This is the bicycle model of the automobile[1], where within the regime of planned driving,

$$\begin{aligned} F_{yf}(t) &\approx -C_y\alpha_f(t) \\ F_{yr}(t) &\approx -C_y\alpha_r(t) \end{aligned}$$

where C_y is the tire stiffness of the tire pairs, and

$$\begin{aligned} \alpha_f(t) &= \arctan\left(\frac{U_y(t)+r(t)a}{U_x(t)}\right)+\delta(t) \\ \alpha_r(t) &= \arctan\left(\frac{U_y(t)-r(t)b}{U_x(t)}\right) \end{aligned}$$

with body fixed longitudinal and lateral velocities, $U_x(t)$ and $U_y(t)$. This models the effect of tires deforming at a rate to provide their force. The differential equations of motion are

$$\begin{aligned} m(\dot{U}_x(t)-r(t)U_y(t)) &= F_{xr}+F_{xf}\cos\delta(t)+F_{yf}\sin\delta(t) \\ m(\dot{U}_y(t)+r(t)U_x(t)) &= F_{yr}-F_{xf}\sin\delta(t)+F_{yf}\cos\delta(t) \\ I_z\dot{r}(t) &= -aF_{xf}(t)\sin\delta(t)+aF_{yf}(t)\cos\delta-bF_{yr}(t) \end{aligned} \tag{3}$$

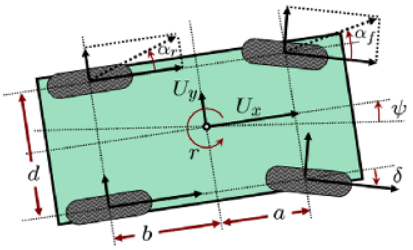

Fig. 3. States of the automobile for the dynamic model.

where $F_{xf}(t)$ and $F_{xr}(t)$ are the components of force provided by the front and rear tires, respectively, in their direction of rolling. The value of C_y was found for the Touareg, with off-road tires, to be 145 $\frac{\text{kN}}{\text{rad}}$, by matching experimental and simulation results, to accurately predict motion.

The steering wheel cannot immediately match the commanded angle. Rather, there is a delay, dependent on the inertia of the steering column, the servo system, and communication delays. Experimentally, a first order model,

$$\dot{\delta}(t) = \tau^{-1}(\delta_c(t) - \delta(t)) \tag{4}$$

was found to accurately model the dynamics seen in the steering wheel's response. The time delay, τ, was 0.4 s for simulation, a conservative value based on experiments.

III. Tracking Control Laws

This section details the lateral and longitudinal control laws. They take the vehicle state and the commanded trajectory as inputs, and output commands at a fixed rate, 20 Hz for Stanley. The estimator, using GPS and inertial sensors, provides the vehicle's state. Only a subset of the commanded trajectory is used: the location, orientation, curvature, and speed of the segment of trajectory closest to the front tires.

A. Lateral Control

This controller provides closed loop tracking of the desired vehicle path, as determined by the path planner, on quickly varying, potentially rough terrain, with resilience to any errors in the state. This section proceeds by determining a partial control law, given the kinematic equations of motion. Then, global asymptotic stability is proven, under the assumption of kinematic motion. Next, the control law is augmented to improve stability and tracking on the real system, by considering the dynamic equations of motion.

By inspecting Equations (1) and (2), a controller is selected such that the resulting differential equation has a globally asymptotically stable equilibrium at zero crosstrack error, as given in Theorem 1.

***Theorem** 1:* For the kinematic equations of motion, given by Equations (1) and (2), using the steering control law,

$$\delta(t) = \begin{cases} \psi(t) + \arctan\frac{k\,e(t)}{v(t)} & \text{if } |\psi(t) + \arctan\frac{k\,e(t)}{v(t)}| < \delta_{max} \\ \delta_{max} & \text{if } \psi(t) + \arctan\frac{k\,e(t)}{v(t)} \geq \delta_{max} \\ -\delta_{max} & \text{if } \psi(t) + \arctan\frac{k\,e(t)}{v(t)} \leq -\delta_{max} \end{cases} \tag{5}$$

results in a closed loop system with a globally asymptotically stable equilibrium at $e = 0$ for $v(t) > 0$ and $0 < \delta_{max} < \frac{\pi}{2}$.

Proof:

Using the steering control law, Equation (5), there are three regions in the phase space of e and ψ – input saturated high, input saturated low, and nominal control, shown in Figure 4. The center region is that under nominal control. Without loss of generality, assume $v(t)$ to be constant. The boundary between regions in phase space is where the nominal steering command, $(\psi(t) + \arctan\frac{k\,e(t)}{v(t)})$, is at the steering limit, so the equation of this boundary, as a function of e, is

$$\psi_b(e) = -\arctan\frac{ke}{v(t)} \pm \delta_{max} \tag{6}$$

For the saturated low region, the phase space trajectories and the boundary line are antisymmetric about the origin to those of the saturated high region. So, without loss of generality, consider the effect of saturation on Equations (1) and (2) in the saturated high region,

$$\begin{aligned} \dot{e}(t) &= v(t)\sin(\psi(t) - \delta_{max}) \\ \dot{\psi}(t) &= -\frac{v(t)\sin(\delta_{max})}{a+b} \end{aligned}$$

Because $\delta_{max} > 0$, $\dot{\psi} < 0$ in this region, and is constant, so $\psi(t)$ decreases linearly with time. In this region, $\psi \leq \pi$, so any state in this region will flow into the nominal region, with boundary given by Equation (6), within finite time.

In the nominal region, substituting Equation (5) into the kinematic equation of motion, Equation (1), yields

$$\dot{e}(t) = -v(t)\sin\arctan\left(\frac{ke(t)}{v(t)}\right) = \frac{-ke(t)}{\sqrt{1+\left(\frac{ke(t)}{v(t)}\right)^2}} \tag{7}$$

Inside the nominal region, the sign of $\dot{e}$ is always opposite that of e, and for any $e(t)$, $|\dot{e}(t)| \in [ke(t), v(t)]$. Thus, the convergence rate of $e(t)$ is between linear, with rate $v(t)$, and exponential, with rate k. Therefore, no orbits can be contained in this region. From Equations (2) and (5), the sign of $\dot{\psi}(t)$ is opposite that of $(\psi(t) + \arctan\frac{k\,e(t)}{v(t)})$, so $\psi(t)$ approaches $\arctan\frac{k\,e(t)}{v(t)}$, which converges to 0. Therefore, the origin is the only stable equilibrium in phase space.

For some values of coefficients, the state can transition from the nominal region to the saturated regions, for sufficiently large $|\dot{e}|$ at the boundary. Transitions occur without chattering along the boundary, because the state time derivative is continuous everywhere except at $\psi = \pm\pi$, which does not intersect the boundary, since $|\psi_b(e)| < \pi \,\forall\, e \in \mathbb{R}$, provided $0 < \delta_{max} < \frac{\pi}{2}$. Any state that flows into the saturated regions will leave in finite time, as already shown. For a transition to the saturated region at time t_1, it must be shown that when the state returns to the nominal region, at time t_2, that $|e(t_2)| < |e(t_1)|$. To show this, note that in this region, $\dot{e}(t)$ is an anti-symmetric function of $\psi(t)$ about $\psi = \delta_{max}$, $\psi(t)$ is linearly decreasing, and $\dot{e}(t) > 0$ when $\psi(t) > \delta_{max}$. Therefore, any state that transitions from the nominal region into the saturated high region will flow to a maximum value of e at $\psi = \delta_{max}$ and return in a path that is symmetric in the

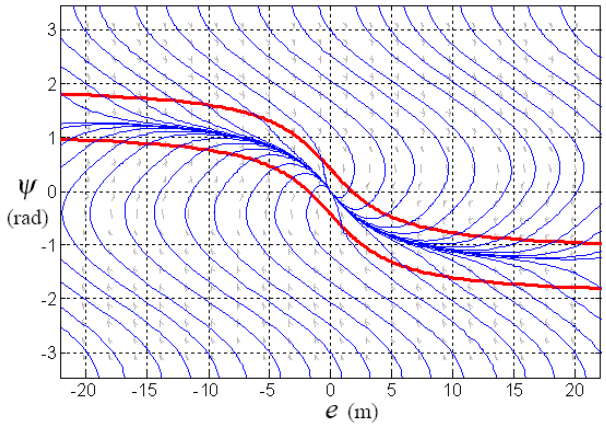

Fig. 4. Phase portrait of a vehicle driving with the steering control law with a speed of $v = 10\ \frac{\text{m}}{\text{s}}$, a gain of $k = 2.5\ \frac{1}{\text{s}}$ and a turning limit of $\delta_{max} = 24°$. The red lines mark the transition from saturated steering, above the top line and below the bottom line, to normal control, between the two lines. In the saturated region, ψ monotonically approaches the normal control region. Inside the normal control region, $|e|$ monotonically decreases.

phase portrait about the line $\psi = \delta_{max}$. Because the boundary defined by Equation (6) is a monotonically decreasing, anti-symmetric function of e about $(\psi, e) = (\delta_{max}, 0)$, when the state flows back into the nominal region across that boundary, on a symmetric path to its departure path, $|e(t_2)| < |e(t_1)|$.

In summary, in the saturated regions, the state transitions to the nominal region in finite time. If the state transitions from the nominal region to a saturated region, it returns to the nominal region in finite time, with a lower value of $|e(t)|$, without chatter on the boundary. In the nominal region, $|e(t)|$ converges with a rate between linear and exponential to the only equilibrium, the origin. Therefore, the origin is the globally asymptotically stable equilibrium of the system. ■

At large crosstrack error, this control law drives the vehicle driving straight toward the trajectory. As crosstrack error becomes small, Equation (7) is approximately $\dot{e}(t) = -ke(t)$, with time domain solution $e(t) = \exp(-kt)$. So, when the vehicle is near the trajectory, it converges to the trajectory exponentially with time constant k. This is a consequence of multiplying k by $\frac{1}{v(t)}$ in the control law, similar to [10]. When the vehicle is facing the wrong direction, the steering command is to turn at δ_{max} in the direction resulting in the shortest path to point forward again. Between these extremes, the arctan function enables a smooth, stable transition.

Using the controller in Equation (5), the location of the front wheels is actively controlled, but the yaw is not. The tires act as dampers, providing reaction forces to sideways velocities. At low speeds, this stabilizes the yaw dynamics, however the magnitude of this reaction is inversely proportional to speed. As speed increases, the damping effect diminishes, creating a need for active damping. Through simulation and experiment, negative feedback on yaw rate was found to provide the best active damping, without impacting tracking performance. Thus, $k_{d,yaw}(r_{meas}(t) - r_{traj}(t))$ is added to the steering command, where $k_{d,yaw}$ is a tuned gain, r_{traj} is the yaw rate for the trajectory, and r_{meas} is the measured yaw rate.

The controller commands a steering servo. Time delay and overshoot in the servo can cause instability. One way to prevent this is to add $k_{d,steer}(\delta_{meas}(i) - \delta_{meas}(i+1))$ to the steering command, where δ_{meas} is the discrete time measurement of the steering angle, and i is the index of the measurement one control period earlier. This provides lead control on the software side. The value of $k_{d,steer}$ is tuned to be large enough to damp the steering wheel response, but small enough to have minimal effect on performance.

Additional attention is required for curvy roads. Automobiles point inward on curves, to generate lateral acceleration with the front *and* rear tires. The controller yaw setpoint should be non-zero. The steady state yaw, ψ_{ss}, relative to a constant curvature path, can be found using sums of forces and moments in Equation (3), yielding

$$\psi_{ss} = \frac{mv(t)r_{traj}(t)}{C_y(1+\frac{a}{b})} = k_{ag}v(t)r_{traj}(t) \tag{8}$$

where $k_{ag} = \frac{m}{C_y(1+\frac{a}{b})}$. In simulations and experiments, using this setpoint in the controller did not impact stability, but did correctly turn the vehicle into turns to null crosstrack error. It does not compensate for transients in trajectory curvature.

One final modification for driving at low speed prevents the gain term $\frac{k}{v(t)}$ from becoming so large that it is oversensitive to noise on $e(t)$. A tuned gain, k_{soft}, is added to the denominator, permitting control to be arbitrarily soft at low speeds. In experiments, $k_{soft} = 1\ \frac{\text{m}}{\text{s}}$ was found appropriate.

The complete steering law, compensating for dynamics, is

$$\begin{aligned}\delta(t) = (\psi(t) - \psi_{ss}(t)) + \arctan\tfrac{k\,e(t)}{k_{soft}+v(t)} \\ +k_{d,yaw}(r_{meas} - r_{traj}) + k_{d,steer}(\delta_{meas}(i) - \delta_{meas}(i+1))\end{aligned} \tag{9}$$

with saturation at $\pm\delta_{max}$. This control law was used without fault on Stanley for hundreds of miles of testing for months prior to the DARPA Grand Challenge race, and in the race. The augmentations to the kinematic control law compensate for dynamics not considered in deriving Equation (5), yielding a controller that is stable and able to null crosstrack error, up to the highest speeds tested—42 mph on a dirt road with Stanley and 71 mph on pavement with Junior.

The same error metric and concepts can be used to steer the vehicle in reverse, by using the rear tires as the guiding wheels, and closing a loop around $\psi(t)$; the orientation of the rear tires. This was implemented and tested on Stanley up to 15 mph off-road, yielding similar performance to [11].

B. Longitudinal Control

The longitudinal controller receives speed requests from: the trajectory planner, a safety speed recommender, and a health monitor. The controller uses the minimum of these speeds as its setpoint. It treats the brake cylinder pressure and throttle level as two opposing, single-acting actuators that exert a longitudinal force on the car. Experiments showed that this is almost exactly true for the brake system. It was found

to be an acceptable simplification of the throttle system. The controller computes a single proportional integral (PI) error metric, at discrete control iteration $i+1$,

$$e_v(i+1) = k_{p,v}(v(i+1) - v_c(i+1)) + k_{i,v}e_{int}(i+1) \quad (10)$$

where the integral term is given by

$$e_{int}(i+1) = e_{int}(i+1) + (v(i+1) - v_c(i+1)) \quad (11)$$

and v_c is the commanded speed. The values of $k_{p,v}$ and $k_{i,v}$ determine the trade-off between disturbance rejection and overshoot. The integral term is saturated to prevent windup.

This opposing, single-acting actuator system can be susceptible to chatter and deadbands, as handled in [12]. Here, a different approach is used, with few modeling assumptions. When the error metric is positive, the brake system commands a brake cylinder pressure proportional to the PI error metric, and when it is negative, the throttle level is set proportional to the negative of the PI error metric. Analysis using a phase portrait [13] demonstrates that this method solves the chatter and deadband problem. To achieve the commanded brake pressure, the control input for the nonlinear, hysteretic brake pressure cylinders is commanded using saturated proportional feedback on the brake pressure.

IV. Experimental Results

Hundred of miles of road tests were conducted using the presented controller between February and October 2005, using the Volkswagen Touareg "Stanley", a 1.9 m wide SUV, with 0.25 m wide off-road tires. Typical speeds were 5 to 35 mph. For details on system architecture, see [14]. The controller ran on a Pentium-M 1.6 GHz computer, consuming negligible resources. For most experiments, humans were in the vehicle to intervene if necessary. Once the initial control system was completed in March 2005, it did not lead to any interventions. The results of several test categories follow.[1]

A. Off-Road Tests

One test took place in the desert in Arizona. The course was a loop of gravel road with erosion on steep grades. See Figure 5 for the course and results. It contained fast straightaways and a winding road that climbs, crests, and descends a steep hillside. The crosstrack error had a mean of 0.003 m, and standard deviation and RMS error of 0.02 m. It contained an obstacle that was swerved around at 25 mph.

Another test took place in the Mojave Desert, at the DARPA Grand Challenge 2004 course. These qualitative results address several scenarios. First, puddles (≥ 0.1 m in depth) were encountered following spring rains. Although they caused sliding, the controller compensated, with maximum crosstrack error of 0.2 to 0.5 m, depending on puddle depth, the road curvature, and the speed. Puddles were traversed up to speeds of 15 mph, covering the windshield in water, but maintaining sub 0.2 m accuracy in straightaways. In dry conditions, as expected, transitions into and out of

[1]Experimental results from Junior are omitted here, as they are preliminary, and for on-road driving. The main preliminary result is the ability to drive up to 71 mph without degradation in accuracy.

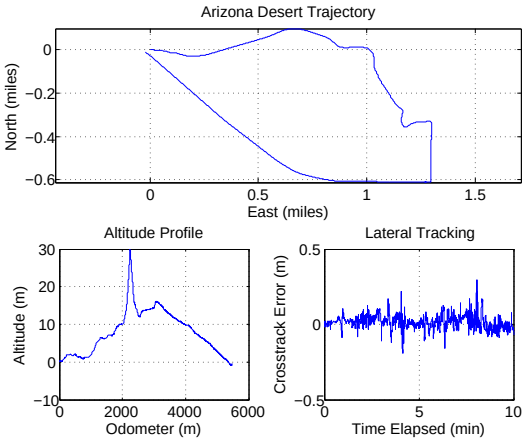

Fig. 5. Stanley log data from a test course in the desert in Arizona. The road was gravel of varying quality. A steep, windy portion in the middle demonstrates tracking on a road with large slopes and erosion.

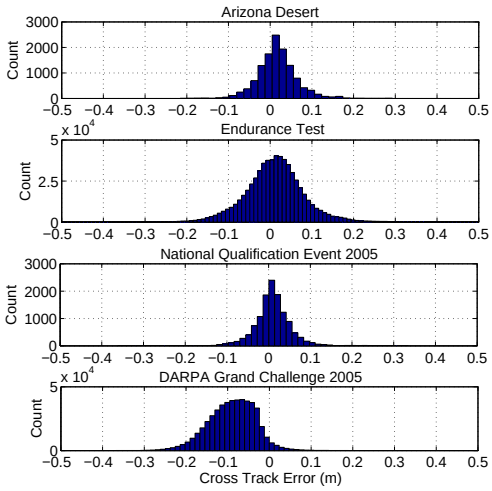

Fig. 6. Histograms of lateral crosstrack errors for various experiments.

curves caused higher crosstrack error, due to the changing angular rate of the trajectory, which is not fed forward into the controller. This was strongly observed when the vehicle swerved around obstacles at 35 mph. Although the rear wheels slid out, the controller kept the front wheels in line with the road, counter steering, as is appropriate. The worst crosstrack error observed in testing was approximately 1.5 m, caused by skidding around a corner on gravel at 20 mph.

B. Endurance Test

This experiment was an endurance test of the vehicle at Volkswagen's Arizona Proving Grounds, on a closed loop dirt track, with obstacles. The loop was 2.3 miles long, and was repeated 88 times, for a total of 200.1 mi of autonomous driving. The mean crosstrack error was 0.02 m, and the RMS crosstrack error and standard deviation were 0.08 m. The results are summarized in Figure 6.

C. DARPA Grand Challenge Desert Race

The DARPA Grand Challenge consisted of the "National Qualification Event" (NQE), at the Ontario Speedway, fol-

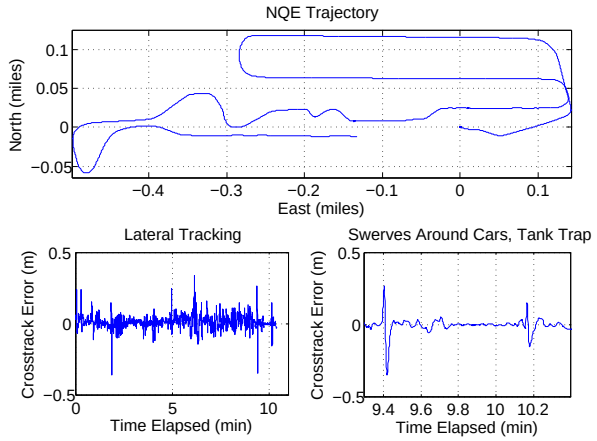

Fig. 7. Stanley log data from the DARPA National Qualification Event 2005. The crosstrack error is zoomed in on the times where Stanley swerved around two parked cars in the middle of the road, and a tank trap, incurring small initial spikes in error with each maneuver, on the order of a tire width.

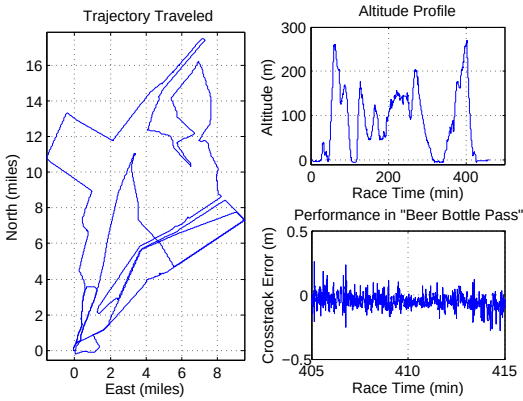

Fig. 8. Stanley log data from the DARPA Grand Challenge 2005. The positions are the estimated vehicle location, and the crosstrack error plot is zoomed in on a critical section of the race, a mountain pass.

lowed by the "Grand Challenge Event" (GCE), a 132 mi race across Nevada desert and mountains, starting and ending in Primm, NV, with no drivers in the vehicles[15]. A chase truck with DARPA officials followed every vehicle, with a remote kill switch. The NQE contained obstacles and simulated difficult terrain. In one characteristic run, shown in Figure 7, the mean crosstrack error was 0.01 m, and the RMS error and standard deviation were 0.05 m. In the GCE, shown in Figure 8, the mean crosstrack error was -0.06 m, the standard deviation was 0.09 m, and the RMS error was 0.1 m. The cause for the larger than normal offset is unknown, but is likely an error in calibration of the steering angle. The offset is only 1/5 the width of a tire. Stanley finished the race in 6 hours, 53 minutes and 58 seconds, averaging 19.1 mph. The maximum speed traveled was 38.0 mph. The 0.1 m RMS error is less than half a tire width, demonstrating the ability to autonomously follow a demanding off-road course with sufficient accuracy to safely track trajectories between hazards, around obstacles, and along cliff edges.

V. Conclusion

A nonlinear control law was presented for an automobile to autonomously track a trajectory, provided in real-time, on rapidly varying off-road terrain, by controlling the orientation of the front wheels with respect to the desired trajectory, enabling collocated control of the system. Global asymptotic stability was proven for the control law, using kinematic equations of motion. Augmentations allow it to handle the dynamics of pneumatic tires and servo-actuated steering. The speed controller uses a switching proportional integral (PI) controller, designed to prevent chatter. The control laws consume negligible computing resources. Experimental results demonstrate the ability to accurately track trajectories in a variety of off-road settings, between hazards, and over rough and curvy roads, with a typical RMS crosstrack error of under 0.1 m. Stanley was the only vehicle not to hit obstacles during the DARPA National Qualification Event, and had the fastest completion time in the DARPA Grand Challenge 2005, averaging 19.1 mph on desert and mountainous terrain.

References

[1] Gillespie, T. D., *Fundamentals of Vehicle Dynamics*, Society of Automotive Engineers, Warrendale, PA, 1992.

[2] Byrne, R. H., Abdallah, C. T., and Dorato, P., "Experimental Results in Robust Lateral Control of Highway Vehicles," *In Proceedings of the 34th Conference on Decision and Control*, New Orleans, LA, December 1995, pp. 3572–3575.

[3] Guldner, J., Sienel, W., Tan, H.-S., and Ackermann, J., "Robust Automatic Steering Control for Look-Down Reference Systems with Front and Rear Sensors," *IEEE Transactions on Control Systems Technology*, Vol. 7, No. 1, January 1999, pp. 2–11.

[4] Rajamani, R., Tan, H.-S., Law, B. K., and Zhang, W.-B., "Demonstration of Integrated Longitudinal and Lateral Control for the Operation of Automated Vehicles in Platoons," *IEEE Transactions on Control Systems Technology*, Vol. 8, No. 4, July 2000, pp. 695–708.

[5] Rossetter, E. J., *A Potential Field Framework for Active Vehicle Lanekeeping Assistance*, PhD Thesis, Stanford University, Dec. 2003.

[6] Gerdes, J. C. and Rossetter, E. J., "A Unified Approach to Driver Assistance Systems Based on Artificial Potential Fields," *Journal of Dynamic Systems, Measurement, and Control*, Vol. 123, No. 3, September 2001, pp. 431–438.

[7] Coombs, D., Murphy, K., Lacaze, A., and Legowik, S., "Driving Autonomously Offroad up to 35 km/h," *In Proceedings of the IEEE Intelligent Vehicles Symposium*, Dearborn, MI, Oct 2000, pp. 186–191.

[8] Kelly, A. and Stentz, A., "Rough Terrain Autonomous Mobility–Part 2: An Active Vision, Predictive Control Approach," *Autonomous Robots*, Vol. 5, No. 2, 1998, pp. 163–198.

[9] O'Connor, M., Bell, T., Elkaim, G., and Parkinson, B., "Automatic Steering of Farm Vehicles Using GPS," *3rd International Conference on Precision Agriculture*, Minneapolis, MN, June 1996.

[10] Broggi, A., Bertozzi, M., Fascioli, A., Bianco, C. G. L., and Piazzi, A., "The ARGO Autonomous Vehicle's Vision and Control Systems," *International Journal of Intelligent Control Systems*, Vol. 3, No. 4, 1999, pp. 409–441.

[11] Patwardhan, S., Tan, H.-S., and Guldner, J., "Lane Following During Backward Driving for Front Wheel Steered Vehicles," *In Proceedings of the American Control Conference*, Albuguerque, NM, June 1997, pp. 3348–3353.

[12] Gerdes, J. C. and Hedrick, J. K., "Hysteresis Control of Nonlinear Single-Acting Actuators as Applied to Brake/Throttle Switching," *In Proceedings of the American Control Conference*, San Diego, CA, June 1999, pp. 1692–1696.

[13] Khalil, H. K., *Nonlinear Systems*, Prentice Hall, 1996.

[14] Thrun, S. et al., "Winning the DARPA Grand Challenge," *Journal of Field Robotics*, Vol. 23, 2006, pp. 661–692.

[15] DARPA, "DARPA Grand Challenge 2005," `http://www.darpa.mil/grandchallenge05/Rules_8oct04.pdf`, 2004.